Global View on Dose Rate Effects in Silica-Based Fibers and Devices Damaged by Radiation-Induced Carrier Trapping

Franck Mady, Mourad Benabdesselam, Jean Bernard Duchez, Yasmine Mebrouk, Sylvain Girard

Global View on Dose Rate Effects in Silica-Based Fibers and Devices Damaged by Radiation-Induced Carrier Trapping

F. Mady[1], M. Benabdesselam[1], J-B. Duchez[1], Y. Mebrouk[1], S. Girard[2]

1. Université de Nice-Sophia Antipolis, LPMC UMR-CNRS 7336, Parc Valrose, 06108 Nice Cedex 2, France

2. Laboratoire Hubert Curien, UMR-CNRS 5516, 42000 Saint-Etienne, France

Abstract (35 words) – We give a global approach clarifying the conditions of enhanced low and high dose rate sensitivity to help in reconciling contradictory results on dose rate dependences. An experimental example on silica optical fibers is presented.

Corresponding and Presenting author:

Franck MADY — Université de Nice-Sophia Antipolis, LPMC UMR CNRS 7336, Parc Valrose, 06108 Nice Cedex 2, France
Phone: +33 4 92 07 63 30; Fax: +33 4 92 07 67 54
franck.mady@unice.fr

Co-authors:

Mourad BENABDESSELAM — Université de Nice Sophia Antipolis; ben@unice.fr
Jean-Bernard DUCHEZ — Université de Nice-Sophia Antipolis; jean-bernard.duchez@unice.fr
Yasmine MEBROUK — Université Nice Sophia Antipolis; yasmine.mebrouk@unice.fr
Sylvain GIRARD — Université de Saint-Etienne; sylvain.girard@univ-st-etienne.fr

Session Preference: Photonic Devices and ICs

Presentation Preference: Oral

I. CONTEXT AND OBJECTIVES

Silica optical fibers and fiber-based sensors are of major interest in a variety of applications in space or nuclear backgrounds. Embedded optical inter-satellite links (OISL) or remote sensing (LIDAR) could e.g. benefit from high power fiber laser sources based on erbium or ytterbium-doped fiber amplifiers that offer the advantages of reduced weight, size, power consumption, cost, and greater efficiency compared with solid-state lasers. The development of the fiber technology is nevertheless limited by radiation-induced darkening, a considerable excess optical loss that develops across the UV, visible and near-IR spectral ranges. By affecting pump (if any) and signal wavelengths, it has dramatic consequences on the performance of fiber-based systems. The design and test of radiation-tolerant fibers have to cope with the dose rate dependence of darkening. This question is notably crucial in space-based applications where the radiation resistance is assessed by accelerated tests, conducted at a much higher dose rate than in actual operation conditions. Beyond the understanding of the dose rate effects, the challenge is to set proper accelerated test protocols.

What we learnt from electronics and Bipolar Junction Transistors (BJTs). Dose rate effects have been a major concern for a long time in electronics, BJTs being for instance very dose rate sensitive. At fixed dose, bipolar components most often exhibit a higher degradation level at low than at high dose rate, this feature being termed "Enhanced Low Dose Rate Sensitivity" (ELDRS). The most elegant ELDRS explanation was proposed in [1]: on the basis of a simple energy level scheme and rate equations, ELDRS was argued to result from the competition between trapping and recombination due to the high concentration of recombination centers in poor quality oxides. The same group also proposed the "dose rate switching" method to conduct accelerated tests on the bipolar technology [2].

The case of erbium-doped fiber amplifiers (EDFA). Evidence for ELDRS in an EDFA, the most common type of fiber amplifier, was recently reported [3]. It motivated an attempt at dose rate switching experiments [4]. A kinetic model proposed in [4] provides simulated switching experiments in qualitative agreement with experimental trends. This model is different from that proposed for BJTs: competition between trapping and recombination is poorly accounted for and dose rate effects are actually controlled by *dispersive detrapping*. However, this point of view implies that the low dose rate degradation is dose-independent for classical non-dispersive kinetics. Trapping-recombination models, where detrapping is not required to produce ELDRS, remain therefore more convincing.

Objectives. Similarities between BJTs and EDFA as regards ELDRS and possible accelerated test routes suggest that electronics and fiber optics may, to a certain extent, receive a joint treatment. Darkening processes in fibers can be cast into trapping-recombination models, as shown by our works [5,6]. Numerical calculations, among which those of [1], have already demonstrated the ability of such models to produce dose rate effects and ELDRS. They were however restricted to a few particular sets of physical parameters and do not state clearly *when and how* the dose rate affects degradation. Given the general importance of this question, especially for space-based applications, and given the contradictory results reported on the dose rate dependence of radiation-induced damage, this work brings original results clarifying the conditions making low dose rate enhance or reduce the degradation in systems where it results from carrier trapping. It also gives operational relationships to estimate the "degradation" in low and high dose rate tails. The notions of "low" and "high" dose rate are defined depending on the defect density and trap polarity. An experimental example is presented.

II. GENERAL MODELING AND OUTCOMES

Model. Figure 1 and equations (1)-(4) present the model under consideration. We focus on dose rate effects arising when trapping and recombination compete under irradiation so thermal release is not considered (as in [1]). Equations are written for electron trapping, but the role of carriers can be readily reversed. To wipe out any particular values and highlight the few determinant parameter ratios, a dimensionless formalism is used. Holes are trapped on recombination centers (RC). Densities of RC and trapped holes are H and h respectively. Electrons can trap on M trapping levels. The kth level has a concentration N_k and is occupied by n_k electrons. Occupancy rates are $\varphi_k = n_k/N_k$ and $\varphi_h = h/H$. The total concentration of electron traps being $N = N_1+N_2+\ldots+N_M$, we use $u_c = n_c/N$ and $u_v = h_v/N$. The weighting of each trapping state is $\xi_k = N_k/N$. Transition ratios, rationalizing the competition between transitions, are $\alpha_k = \beta_k/\gamma$, $\theta = \delta/\gamma$ and $r = H/N$.

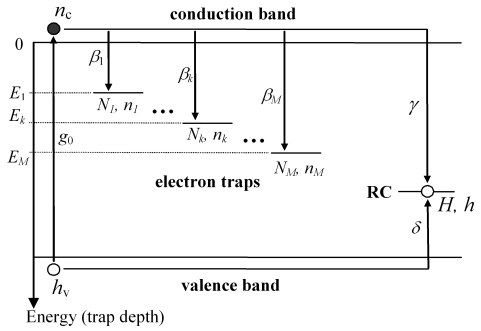

Figure 1. Energy level model with its transition parameters. RC = recombination centers (hole traps).

$$\frac{du_c}{d\tau} = R - u_c \sum_{k=1}^{M} \alpha_k \xi_k \left(1-\varphi_k\right) - r u_c \varphi_h, \qquad (1)$$

$$\frac{d\varphi_k}{d\tau} = \alpha_k u_c \left(1-\varphi_k\right),\ k = 1..M, \qquad (2)$$

$$\frac{du_v}{d\tau} = R - \theta r u_v \left(1-\varphi_h\right), \qquad (3)$$

$$\frac{d\varphi_h}{d\tau} = \theta u_v \left(1-\varphi_h\right) - u_c \varphi_h. \qquad (4)$$

$R = g_0/\gamma N^2$ is the dimensionless dose rate, where g_0 is the generation rate in $cm^{-3}\ s^{-1}$. For a t_0 irradiation duration, the total density of created electron-hole pairs (EHP) is $N_{ehp} = g_0 \times t_0$. We therefore define $D = N_{ehp}/N$ to be the dimensionless dose (taking $D << 1$ keeps the system far below trap saturation). If time is denoted by t, the reduced time is $\tau = \gamma N t$. In such models, *the degradation is represented by the amount of trapped charge*. This assumption directly holds for fibers since darkening develops due to the radiation-induced release of free carriers that subsequently trap on defects to form color centers responsible for optical absorption. The picture is more incomplete for BJTs whose degradation further involves the migration of the protons released upon hole trapping to a Si/SiO_2 interface. Migration would require drift or diffusion whereas equations (1)-(4) (and those in [1]) do not include transport terms and therefore describe a field-free, spatially homogeneous material.

Key lessons. The dimensionless treatment shows that steady-state trap occupancy rates (SSOR) obtained after irradiation are entirely governed by the M+2 dimensionless ratios $\alpha_k = \beta_k/\gamma$, $\theta = \delta/\gamma$ and $r = H/N$. These ratios indeed determine the recombination efficiency with respect to trapping. In the limit case $\theta >> 1$ and $r >> 1$ (recombination is neither limited by a weak hole trapping nor by a weak density of RC) SSOR are only governed by α_k. Then, they can be exactly calculated as a function of the dose at both dose rate limits ($R \rightarrow 0$ and $R \rightarrow \infty$). We found:

$$D = \sum_{k=1}^{M} \xi_k \left(1-\left(1-\varphi_{p_{eq}}\right)^{\alpha_k/\alpha_p}\right) \Big/ \left(1-\varphi_{p_{eq}}\right)^{1/\alpha_p};\ p = 1..M, \text{ for } R \rightarrow \infty \qquad (5)$$

$$D = \sum_{k=1}^{M} \xi_k \left(1-\frac{1}{\alpha_k}\right)\left(1-\left(1-\varphi_{p_{eq}}\right)^{\alpha_k/\alpha_p}\right) - \frac{1}{\alpha_p}\ln\left(1-\varphi_{p_{eq}}\right);\ p = 1..M, \text{ for } R \rightarrow 0 \qquad (6)$$

Given the material parameters ξ_k and α_k ($k = 1..M$), these equations give the dose D required to achieve a SSOR φ_{peq} for the pth trap. More simple forms are obtained if traps have a same capture cross section ($\beta_k = \beta$ and $\alpha_k = \alpha$). In this case $\varphi_k = \varphi$ for transient and SSOR values, and:

$$D = \varphi_{eq} \Big/ \left(1-\varphi_{eq}\right)^{\frac{1}{\alpha}} \text{ for } R \rightarrow \infty \quad \text{and} \quad D = \left(1-\frac{1}{\alpha}\right)\varphi_{eq} - \frac{1}{\alpha}\ln\left(1-\varphi_{eq}\right) \text{ for } R \rightarrow 0$$

By comparing equations (5) and (6), or their simplified form, it is readily demonstrated that SSOR are always higher at the low dose rate limit than at very high dose rate: an ELDRS is always produced for $\theta >> 1$ and $r >> 1$. The ELDRS amplitude is negligible for $\alpha \geq 1$. It increases dramatically as α is decreased below 1 (more efficient recombination). When the recombination efficiency is limited by a weak hole trapping probability ($r >> 1$ but $\theta \leq 1$), SSOR are still given by equation (6) for the low dose rate limit because EHP injection remains the slowest (so the limiting) process. At high dose rate, numerical calculations indicate that SSOR follow equation (5) at low doses ($D < 10\theta$ approximately). At higher doses, SSOR grows towards unity (saturation) much faster than predicted by equation (5). A crossover then appears between the high dose rate SSOR and the θ-independent SSOR at $R \rightarrow 0$ (the smaller θ, the lower the crossover dose): higher trap occupancies can be achieved at higher dose rates!

When hole trapping and recombination is limited by RC saturation ($\theta >> 1$ but $r \leq 1$), SSOR are still given by (5) and (6) if $D << r$ at both dose rate limits because RC can not be saturated as long as $N_{ehp} << H$. When $D > r$, RC saturation can occur. Equations (5) and (6) underestimate SSOR that increase faster towards trap saturation. Logically, RC saturation first appears at high R, but the low dose rate SSOR also start to deviate above the values given by equation (6). Both SSOR merge into one curve obeying $D = \varphi_{eq} - r/\alpha \times \ln(1-\varphi_{eq})$ (for a single α) when RC saturation is completed. In fact, ELDRS is the only possible feature for $\theta >> 1$ and $r \leq 1$, but its amplitude is less important than that obtained for $\theta >> 1$ and $r >> 1$. It moreover affects a much narrower dose range.

Figure 2 displays the relative difference Δ (in %) between SSOR obtained for $R \rightarrow 0$ and $R \rightarrow \infty$ respectively as a function of the dose. Positive Δ reveal ELDRS whereas negative Δ are obtained for enhanced SSOR at high dose rate. These plots have been calculated for $\alpha = 10^{-4}$, $\theta = 10^{-2}$ and $r = 2$, 7, 20, and 100. They well illustrate that (*i*) The dose rate dependence is not an intrinsic property of the system; the sign and magnitude of Δ strongly depend on the dose, (*ii*) As regards the concentration of RC, the determining parameter is not H but $r = H/N$. Dose rate effects increase with r and ELDRS prevails at high r values. Therefore ELDRS exhibited by BJTs should not be attributed to the poor quality of the oxide. Indeed, if low-quality silica has a high density of RC (high H), it should also present a high density of trapping states N and hence rather small r values. The point is that ELDRS is the most common feature inherent systems involving trapping and recombination. The *enhanced high dose rate sensitivity* is the signature of an indirect recombination process *at least* limited by a weak probability of trapping on RC ($\theta \leq 1$).

"Low" and "High" dose rate regions. Basically, a low dose rate exposure refers to a situation where EHP can trap faster than they are created. For doses $D < 1$, traps are not saturated and the trapping rate is roughly βN (for a single β). The generation rate per unit trap density being g_0/N (in s^{-1}), a sufficient condition to meet this criterion is $g_0/N << \beta N$ or $R << \alpha$ in dimensionless form. Therefore a critical dose rate is $g_{0Crit} = \beta N^2$. As D approaches 1, the trapping rate decreases due to trap filling and g_{0Crit} is moderately shifted above βN^2. Figure 3 localizes the critical dose rate βN^2. The latter lies in the grey region delimited by the reasonable lower and upper order of magnitudes of β expected for trapping of electrons, i.e. $10^{-11} < \beta < 10^{-7}$ cm^3 s^{-1}. Dose rates have been converted in rad h^{-1} by using the generation efficiency $G \sim 5.2 \times 10^{12}$ EHP cm^{-3} rad^{-1} in silica.

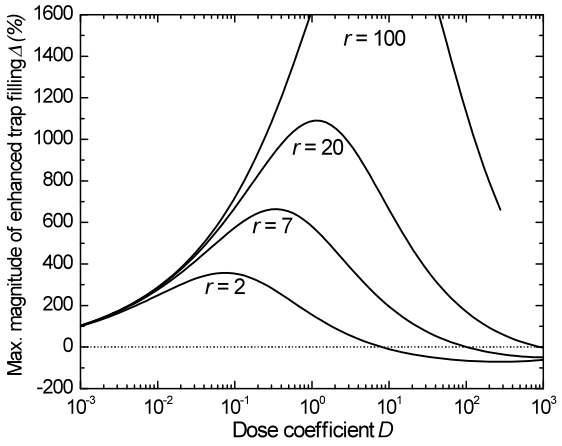

Figure 2. Maximum SSOR enhancement Δ as a function of the reduced dose D (see text).

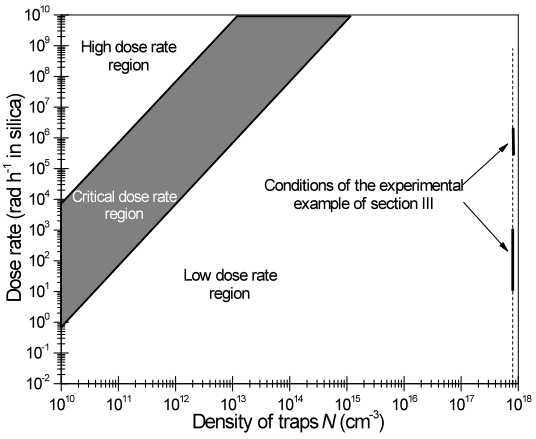

Figure 3. Typical low dose rate, high dose rate and the critical dose rate (βN^2) regions for electron trapping.

III. EXPERIMENTAL EXAMPLE

Germanosilicate fibers are the standard passive fibers for signal transmission (1550 nm). Radiation-induced optically active centers in such fibers mainly consist of the so-called Ge(1) and Ge(2) centers that are formed upon electron trapping under irradiation [7,8]. We investigated the dose rate dependence of trap filling in various germanosilicate fibers produced by iXFiber SAS. Three types of fiber samples, named GeD1, GeD2 and GeD3, have been drawn from the same preform at 3 drawing speeds for research purposes (ref. [8,9] are already based on similar samples). Details about these fibers can be found in [8]. According to [8] the total density of electron traps, acting as precursors of

Ge(1) and Ge(2) centers, is N~8-9×10^{17} cm^{-3}. The samples were submitted to 10, 50 and 100 krad gamma irradiations (^{60}Co) at 30, 100 and 500 rad h^{-1}. Much higher dose rates (2.18×10^5 and 2,63×10^6 rad h^{-1}) were also obtained from a 45 kV x-ray generator. Trap filling, i.e. the cumulated Ge(1) and Ge(2) concentration, was estimated by thermally stimulated luminescence (TSL). The TSL glow curves from GeD1, 2 and 3, have a single broad peak around 250 °C. TSL readouts (between room temperature and 450°C at 2 °C s^{-1}) were found to empty all traps and to result in full bleaching. In these conditions, integrated TSL responses are proportional to the trap SSOR. Figure 4 presents, in arbitrary units, the "measured" SSOR. No clear dose rate dependence is established aside from measurement errors and sample variations. Results obtained after x-ray exposure are systematically higher than those measured after gamma irradiation. This should not be considered a dose rate effect since gamma and x-ray irradiations were not been conducted in the same conditions. The thermal annealing of radiation-induced defects in GeD1-3 is about 5% in 8 hours at room temperature [9] (this weak value is consistent with section II, where thermal release is neglected within the time required to reach SSOR). Gamma irradiations and TSL experiments were separated by more than 2 months whereas TSL readouts were performed right after x-ray exposures, in the same laboratory.

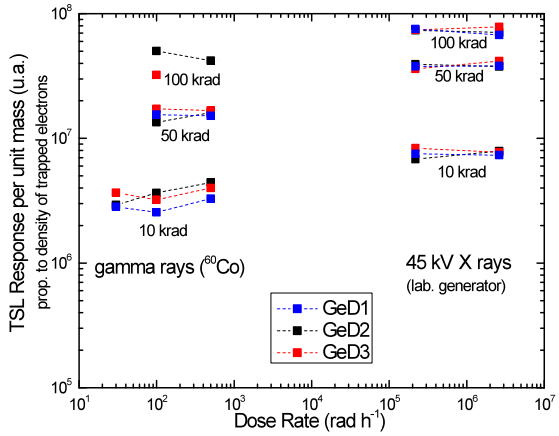

Figure 4. SSOR "measured" by TSL

The used dose rate ranges, together with the estimated trap density, are reported in figure 3. The doses imparted in our experiments did not saturate traps (saturation at 10^6 rad [8]). We therefore met the condition $D < 1$ and βN^2 is well the relevant critical dose rate, as assumed in figure 3. According to this figure, all of our irradiations come into the low dose rate tail, in agreement with the rather dose rate independent measured SSOR. Contrary to what happens to EDFA [3,4], the low dose rate region here embraces the routine laboratory irradiation conditions, rendering accelerated protocols unnecessary for germanosilicate fibers.

IV. CONCLUSION

We give an original, most general treatment to a standard model that is directly relevant or readily adjustable to account for dose rate effects in optical fibers but that is also still useful for electronics. Taking this step back is important to enlighten some experimental behaviors and interpretations. For instance, the fact that an EDFA shows ELDRS at reachable dose rates (50 and 1200 rad h^{-1} in [4]) indicates that carriers involved in the degradation are most likely trapped holes. Holes indeed have a very low mobility in silica and their trapping is characterized by very low β values. This makes the grey stripe of the critical dose rate region slide down towards the right bottom corner of figure 3. Then, experimental dose rates can come into the transition region around g_{0Crit} at plausible density of traps (10^{15}-10^{18} cm^{-3}) so dose rate effects can be observed. By the way, BJT degradation involves hole trapping, and dose rate effects are observed… We also remind that comparison between dose rate dependences of the degradation of similar fibers (or other relevant systems) should consider differences in experimental conditions (the dose e.g.) or in dopant concentrations.

REFERENCES

[1] J. Boch, F. Saigné, A. D. Touboul, S. Ducret, J-F. Carlotti, M. Bernard, R.D. Schrimpf, F. Wrobel, and G. Sarrabayrouse, Appl. Phys. Lett., 88 (2006), 232113

[2] J. Boch, F. Saigné, R.D. Schrimpf, J-R. Vaillé, L. Dusseau,S. Ducret, M. Bernard, E. Lorfèvre, and C. Chatry, IEEE Trans. Nucl. Sci., 52 (2005), p. 2616

[3] B. Brichard, A. Fernandez Fernandez, H. Ooms, and F. Berghmans, OFS-16: 16th Int. Conf. on optical fiber sensors, 336

[4] O. Gilard, J. Thomas, L. Trousselier, M. Myara, P. Signoret, E. Burov, and M. Sotom, Appl. Opt., 51 (2012), p. 2230

[5] F. Mady, M. Benabdesselam, Y. Mebrouk and D. Dussardier, Proc. RADECS 2010, paper LN2

[6] F. Mady, M. Benabdesselam, and W. Blanc, Opt. Lett., 35 (2010), p. 3541

[7] D. Griscom, Opt. Mat. Express, 1 (2011), p. 400

[8] A. Alessi, S. Girard, C. Macandella, S. Agnello, M. Cannas, A. Boukenter, and Y. Ouerdane, Journal of Non-Crystalline Solids, 357 (2011), p. 1966.

[9] M. Benabdessselam, F. Mady, and S. Girard, Journal of Non-Crystalline Solids 360 (2013), p. 9